

Partonic Flow and ϕ -Meson Production in Au + Au Collisions at $\sqrt{s_{NN}} = 200$ GeV

B. I. Abelev,⁹ M. M. Aggarwal,³⁰ Z. Ahammed,⁴⁵ B. D. Anderson,²⁰ D. Arkhipkin,¹³ G. S. Averichev,¹² Y. Bai,²⁸ J. Balewski,¹⁷ O. Barannikova,⁹ L. S. Barnby,² J. Baudot,¹⁸ S. Baumgart,⁵⁰ V. V. Belaga,¹² A. Bellingeri-Laurikainen,⁴⁰ R. Bellwied,⁴⁸ F. Benedosso,²⁸ R. R. Betts,⁹ S. Bhardwaj,³⁵ A. Bhasin,¹⁹ A. K. Bhati,³⁰ H. Bichsel,⁴⁷ J. Bielcik,⁵⁰ J. Bielcikova,⁵⁰ L. C. Bland,³ S.-L. Blyth,²² M. Bombara,² B. E. Bonner,³⁶ M. Botje,²⁸ J. Bouchet,⁴⁰ A. V. Brandin,²⁶ A. Bravar,³ T. P. Burton,² M. Bystersky,¹¹ R. V. Cadman,¹ X. Z. Cai,³⁹ H. Caines,⁵⁰ M. Calderón de la Barca Sánchez,⁶ J. Callner,⁹ O. Catu,⁵⁰ D. Cebra,⁶ Z. Chajecski,²⁹ P. Chaloupka,¹¹ S. Chattopadhyay,⁴⁵ H. F. Chen,³⁸ J. H. Chen,³⁹ J. Y. Chen,⁴⁹ J. Cheng,⁴³ M. Cherney,¹⁰ A. Chikanian,⁵⁰ W. Christie,³ S. U. Chung,³ J. P. Coffin,¹⁸ T. M. Cormier,⁴⁸ M. R. Cosentino,³⁷ J. G. Cramer,⁴⁷ H. J. Crawford,⁵ D. Das,⁴⁵ S. Dash,¹⁵ M. Daugherty,⁴² M. M. de Moura,³⁷ T. G. Dedovich,¹² M. DePhillips,³ A. A. Derevschikov,³² L. Didenko,³ T. Dietel,¹⁴ P. Djawotho,¹⁷ S. M. Dogra,¹⁹ X. Dong,²² J. L. Drachenberg,⁴¹ J. E. Draper,⁶ F. Du,⁵⁰ V. B. Dunin,¹² J. C. Dunlop,³ M. R. Dutta Mazumdar,⁴⁵ V. Eckardt,²⁴ W. R. Edwards,²² L. G. Efimov,¹² V. Emelianov,²⁶ J. Engelage,⁵ G. Eppley,³⁶ B. Erasmus,⁴⁰ M. Estienne,¹⁸ P. Fachini,³ R. Fatemi,²³ J. Fedorisin,¹² A. Feng,⁴⁹ P. Filip,¹³ E. Finch,⁵⁰ V. Fine,³ Y. Fisyak,³ J. Fu,⁴⁹ C. A. Gagliardi,⁴¹ L. Gaillard,² M. S. Ganti,⁴⁵ E. Garcia-Solis,⁹ V. Ghazikhanian,⁷ P. Ghosh,⁴⁵ Y. G. Gorbunov,¹⁰ H. Gos,⁴⁶ O. Grebenyuk,²⁸ D. Grosnick,⁴⁴ B. Grube,³⁴ S. M. Guertin,⁷ K. S. F. F. Guimaraes,³⁷ N. Gupta,¹⁹ B. Haag,⁶ T. J. Hallman,³ A. Hamed,⁴¹ J. W. Harris,⁵⁰ W. He,¹⁷ M. Heinz,⁵⁰ T. W. Henry,⁴¹ S. Heppelmann,³¹ B. Hippolyte,¹⁸ A. Hirsch,³³ E. Hjort,²² A. M. Hoffman,²³ G. W. Hoffmann,⁴² D. J. Hofman,⁹ R. S. Hollis,⁹ M. J. Horner,²² H. Z. Huang,⁷ E. W. Hughes,⁴ T. J. Humanic,²⁹ G. Igo,⁷ A. Iordanova,⁹ P. Jacobs,²² W. W. Jacobs,¹⁷ P. Jakl,¹¹ F. Jia,²¹ P. G. Jones,² E. G. Judd,⁵ S. Kabana,⁴⁰ K. Kang,⁴³ J. Kapitan,¹¹ M. Kaplan,⁸ D. Keane,²⁰ A. Kechechyan,¹² D. Kettler,⁴⁷ V. Yu. Khodyrev,³² B. C. Kim,³⁴ J. Kiryluk,²² A. Kisiel,⁴⁶ E. M. Kislov,¹² S. R. Klein,²² A. G. Knospe,⁵⁰ A. Kocoloski,²³ D. D. Koetke,⁴⁴ T. Kollegger,¹⁴ M. Kopytine,²⁰ L. Kotchenda,²⁶ V. Kouchpil,¹¹ K. L. Kowalik,²² P. Kravtsov,²⁶ V. I. Kravtsov,³² K. Krueger,¹ C. Kuhn,¹⁸ A. I. Kulikov,¹² A. Kumar,³⁰ P. Kurnadi,⁷ A. A. Kuznetsov,¹² M. A. C. Lamont,⁵⁰ J. M. Landgraf,³ S. Lange,¹⁴ S. LaPointe,⁴⁸ F. Laue,³ J. Lauret,³ A. Lebedev,³ R. Lednicky,¹³ C.-H. Lee,³⁴ S. Lehocka,¹² M. J. LeVine,³ C. Li,³⁸ Q. Li,⁴⁸ Y. Li,⁴³ G. Lin,⁵⁰ X. Lin,⁴⁹ S. J. Lindenbaum,²⁷ M. A. Lisa,²⁹ F. Liu,⁴⁹ H. Liu,³⁸ J. Liu,³⁶ L. Liu,⁴⁹ T. Ljubicic,³ W. J. Llope,³⁶ R. S. Longacre,³ W. A. Love,³ Y. Lu,⁴⁹ T. Ludlam,³ D. Lynn,³ G. L. Ma,³⁹ J. G. Ma,⁷ Y. G. Ma,³⁹ D. P. Mahapatra,¹⁵ R. Majka,⁵⁰ L. K. Mangotra,¹⁹ R. Manweiler,⁴⁴ S. Margetis,²⁰ C. Markert,⁴² L. Martin,⁴⁰ H. S. Matis,²² Yu. A. Matulenko,³² C. J. McClain,¹ T. S. McShane,¹⁰ Yu. Melnick,³² A. Meschanin,³² J. Millane,²³ M. L. Miller,²³ N. G. Minaev,³² S. Mioduszewski,⁴¹ C. Mironov,²⁰ A. Mischke,²⁸ J. Mitchell,³⁶ B. Mohanty,²² D. A. Morozov,³² M. G. Munhoz,³⁷ B. K. Nandi,¹⁶ C. Nattrass,⁵⁰ T. K. Nayak,⁴⁵ J. M. Nelson,² C. Nepali,²⁰ P. K. Netrakanti,³³ L. V. Nogach,³² S. B. Nurushev,³² G. Odyniec,²² A. Ogawa,³ V. Okorokov,²⁶ M. Oldenburg,²² D. Olson,²² M. Pachr,¹¹ S. K. Pal,⁴⁵ Y. Panebratsev,¹² A. I. Pavlinov,⁴⁸ T. Pawlak,⁴⁶ T. Peitzmann,²⁸ V. Perevoztchikov,³ C. Perkins,⁵ W. Peryt,⁴⁶ S. C. Phatak,¹⁵ M. Planinic,⁵¹ J. Pluta,⁴⁶ N. Poljak,⁵¹ N. Porile,³³ A. M. Poskanzer,²² M. Potekhin,³ E. Potrebenikova,¹² B. V. K. S. Potukuchi,¹⁹ D. Prindle,⁴⁷ C. Pruneau,⁴⁸ J. Putschke,²² I. A. Qattan,¹⁷ R. Raniwala,³⁵ S. Raniwala,³⁵ R. L. Ray,⁴⁰ D. Relyea,⁴ A. Ridiger,²⁶ H. G. Ritter,²² J. B. Roberts,³⁶ O. V. Rogachevskiy,¹² J. L. Romero,⁶ A. Rose,²² C. Roy,⁴⁰ L. Ruan,²² M. J. Russcher,²⁸ R. Sahoo,¹⁵ I. Sakrejda,²² T. Sakuma,²³ S. Salur,⁵⁰ J. Sandweiss,⁵⁰ M. Sarsour,⁴¹ P. S. Sazhin,¹² J. Schambach,⁴² R. P. Scharenberg,³³ N. Schmitz,²⁴ J. Seger,¹⁰ I. Selyuzhenkov,⁴⁸ P. Seyboth,²⁴ A. Shabetai,¹⁸ E. Shahaliev,¹² M. Shao,³⁸ M. Sharma,³⁰ W. Q. Shen,³⁹ S. S. Shimanskiy,¹² E. P. Sichtermann,²² F. Simon,²³ R. N. Singaraju,⁴⁵ N. Smirnov,⁵⁰ R. Snellings,²⁸ P. Sorensen,³ J. Sowinski,¹⁷ J. Speltz,¹⁸ H. M. Spinka,¹ B. Srivastava,³³ A. Stadnik,¹² T. D. S. Stanislaus,⁴⁴ D. Staszak,⁷ R. Stock,¹⁴ M. Strikhanov,²⁶ B. Stringfellow,³³ A. A. P. Suaide,³⁷ M. C. Suarez,⁹ N. L. Subba,²⁰ M. Sumner,¹¹ X. M. Sun,²² Z. Sun,²¹ B. Surrow,²³ T. J. M. Symons,²² A. Szanto de Toledo,³⁷ J. Takahashi,³⁷ A. H. Tang,³ T. Tarnowsky,³³ J. H. Thomas,²² A. R. Timmins,² S. Timoshenko,²⁶ M. Tokarev,¹² T. A. Trainor,⁴⁷ S. Trentalange,⁷ R. E. Tribble,⁴¹ O. D. Tsai,⁷ J. Ulery,³³ T. Ullrich,³ D. G. Underwood,¹ G. Van Buren,³ N. van der Kolk,²⁸ M. van Leeuwen,²² A. M. Vander Molen,²⁵ R. Varma,¹⁶ I. M. Vasilevski,¹³ A. N. Vasiliev,³² R. Vernet,¹⁸ S. E. Vigdor,¹⁷ Y. P. Viyogi,¹⁵ S. Vokal,¹² S. A. Voloshin,⁴⁸ W. T. Waggoner,¹⁰ F. Wang,³³ G. Wang,⁷ J. S. Wang,²¹ X. L. Wang,³⁸ Y. Wang,⁴³ J. W. Watson,²⁰ J. C. Webb,⁴⁴ G. D. Westfall,²⁵ A. Wetzler,²² C. Whitten, Jr.,⁷ H. Wieman,²² S. W. Wissink,¹⁷ R. Witt,⁵⁰ J. Wu,³⁸ Y. Wu,⁴⁹ N. Xu,²² Q. H. Xu,²² Z. Xu,³ P. Yepes,³⁶ I.-K. Yoo,³⁴ Q. Yue,⁴³ V. I. Yurevich,¹² W. Zhan,²¹ H. Zhang,³ W. M. Zhang,²⁰ Y. Zhang,³⁸ Z. P. Zhang,³⁸ Y. Zhao,³⁸ C. Zhong,³⁹ J. Zhou,³⁶ R. Zoukarniev,¹³ Y. Zoukarnieva,¹³ A. N. Zubarev,¹² and J. X. Zuo³⁹

(STAR Collaboration)

- ¹Argonne National Laboratory, Argonne, Illinois 60439, USA
²University of Birmingham, Birmingham, United Kingdom
³Brookhaven National Laboratory, Upton, New York 11973, USA
⁴California Institute of Technology, Pasadena, California 91125, USA
⁵University of California, Berkeley, California 94720, USA
⁶University of California, Davis, California 95616, USA
⁷University of California, Los Angeles, California 90095, USA
⁸Carnegie Mellon University, Pittsburgh, Pennsylvania 15213, USA
⁹University of Illinois at Chicago, Chicago, Illinois 60607, USA
¹⁰Creighton University, Omaha, Nebraska 68178, USA
¹¹Nuclear Physics Institute AS CR, 250 68 Řež/Prague, Czech Republic
¹²Laboratory for High Energy (JINR), Dubna, Russia
¹³Particle Physics Laboratory (JINR), Dubna, Russia
¹⁴University of Frankfurt, Frankfurt, Germany
¹⁵Institute of Physics, Bhubaneswar 751005, India
¹⁶Indian Institute of Technology, Mumbai, India
¹⁷Indiana University, Bloomington, Indiana 47408, USA
¹⁸Institut de Recherches Subatomiques, Strasbourg, France
¹⁹University of Jammu, Jammu 180001, India
²⁰Kent State University, Kent, Ohio 44242, USA
²¹Institute of Modern Physics, Lanzhou, China
²²Lawrence Berkeley National Laboratory, Berkeley, California 94720, USA
²³Massachusetts Institute of Technology, Cambridge, Massachusetts 02139-4307, USA
²⁴Max-Planck-Institut für Physik, Munich, Germany
²⁵Michigan State University, East Lansing, Michigan 48824, USA
²⁶Moscow Engineering Physics Institute, Moscow Russia
²⁷City College of New York, New York City, New York 10031, USA
²⁸NIKHEF and Utrecht University, Amsterdam, The Netherlands
²⁹Ohio State University, Columbus, Ohio 43210, USA
³⁰Panjab University, Chandigarh 160014, India
³¹Pennsylvania State University, University Park, Pennsylvania 16802, USA
³²Institute of High Energy Physics, Protvino, Russia
³³Purdue University, West Lafayette, Indiana 47907, USA
³⁴Pusan National University, Pusan, Republic of Korea
³⁵University of Rajasthan, Jaipur 302004, India
³⁶Rice University, Houston, Texas 77251, USA
³⁷Universidade de Sao Paulo, Sao Paulo, Brazil
³⁸University of Science & Technology of China, Hefei 230026, China
³⁹Shanghai Institute of Applied Physics, Shanghai 201800, China
⁴⁰SUBATECH, Nantes, France
⁴¹Texas A&M University, College Station, Texas 77843, USA
⁴²University of Texas, Austin, Texas 78712, USA
⁴³Tsinghua University, Beijing 100084, China
⁴⁴Valparaiso University, Valparaiso, Indiana 46383, USA
⁴⁵Variable Energy Cyclotron Centre, Kolkata 700064, India
⁴⁶Warsaw University of Technology, Warsaw, Poland
⁴⁷University of Washington, Seattle, Washington 98195, USA
⁴⁸Wayne State University, Detroit, Michigan 48201, USA
⁴⁹Institute of Particle Physics, CCNU (HZNU), Wuhan 430079, China
⁵⁰Yale University, New Haven, Connecticut 06520, USA
⁵¹University of Zagreb, Zagreb, HR-10002, Croatia

(Received 20 March 2007; published 11 September 2007)

We present first measurements of the ϕ -meson elliptic flow ($v_2(p_T)$) and high-statistics p_T distributions for different centralities from $\sqrt{s_{NN}} = 200$ GeV Au + Au collisions at RHIC. In minimum bias collisions the v_2 of the ϕ meson is consistent with the trend observed for mesons. The ratio of the yields of the Ω to those of the ϕ as a function of transverse momentum is consistent with a model based on the recombination of thermal s quarks up to $p_T \sim 4$ GeV/ c , but disagrees at higher momenta. The nuclear modification factor (R_{CP}) of ϕ follows the trend observed in the K_S^0 mesons rather than in Λ baryons, supporting baryon-meson scaling. These data are consistent with ϕ mesons in central Au + Au collisions being created via coalescence of thermalized s quarks and the formation of a hot and dense matter with partonic collectivity at RHIC.

The primary aim of ultrarelativistic heavy-ion collisions is to produce and study a state of high-density nuclear matter called the quark-gluon plasma (QGP), the existence of which is supported by lattice QCD calculations [1–3]. Indeed, the experimental results have demonstrated the formation of hot and dense matter in high-energy nuclear collisions at RHIC [4]. In the search for this new form of matter, penetrating probes are essential in order to gain information from the earliest stage of the collisions. A phenomenological analysis [5] has suggested a relatively small hadronic interaction cross section for ϕ -mesons although discussions about the ϕ -proton interaction cross section are yet to be conclusive [6,7]. Therefore ϕ -mesons from high-energy nuclear collisions are expected to provide information about the early partonic stages of the system's evolution since they should remain mostly unaffected by hadronic interactions. This is further supported by recent measurements [8] which have ruled out the idea of ϕ -meson production by kaon coalescence.

Elliptic flow, v_2 , is an observable which is thought to reflect conditions from the early stage of the collision [9,10]. In noncentral heavy-ion collisions, the initial spatial anisotropy of the overlap region of the colliding nuclei is transformed into an anisotropy in momentum space through interactions between the particles. Systematic measurements of the v_2 for the strange hadrons K_S^0 , Λ , Ξ , and Ω suggest that collectivity is developed at the partonic stage at RHIC [11,12]. The evidence for partonic collectivity, one of the conditions for QGP formation, will be further strengthened if it can be shown that ϕ -mesons flow like the other mesons.

A mass ordering predicted by hydrodynamics [13–15] for $v_2(p_T)$ of identified particles has been observed for $p_T \leq 2$ GeV/c. At intermediate transverse momentum, $2 \leq p_T \leq 5$ GeV/c, a separation of baryons and mesons has been observed in measurements of both v_2 and the nuclear modification factor, R_{CP} [12,16,17]. These results are consistent with calculations from quark recombination models [18–21] that assume the deconfinement of the system prior to hadronization. The ϕ is a vector meson, comparable in mass to the proton and Λ baryons with a relatively long lifetime. Its v_2 and R_{CP} will provide a critical test of the assumed underlying dynamics. In addition, as argued in [22], the ratio of the Ω -baryon over ϕ -meson yields can be used to test the nature of light-quark thermalization in the medium. In the model, ϕ s and Ω s are formed via the coalescence of the thermalized quarks at low p_T . The model predicts that the ratio of the Ω to ϕ yields will rise monotonically in low p_T region.

The results presented in this Letter were obtained with the STAR detector [23] at the Relativistic Heavy-Ion Collider (RHIC) at Brookhaven National Laboratory. The detector components used in this analysis were the time

projection chamber (TPC), and trigger detectors, namely, the zero degree calorimeters. Central collisions were selected using the central trigger barrel. The collision centrality was determined by the charged hadron multiplicity within pseudorapidity $|\eta| < 0.5$.

High-statistics Au + Au data were taken in the 2004 run at $\sqrt{s_{NN}} = 200$ GeV. The minimum bias data set used in this analysis consisted of ~ 13.5 million events and the central-triggered data set comprised about 10×10^6 events. Events were required to have a primary vertex z position (where z is the direction of the beam axis) within 30 cm of the center of the TPC. Events from the minimum bias data set were divided into 8 centrality bins: 0%–10%, 10%–20%, 20%–30%, 30%–40%, 40%–50%, 50%–60%, 60%–70%, and 70%–80% of the measured cross section. The central-triggered data set was used to extract the 0%–5% and 0%–12% data.

The ϕ yield in each p_T bin was extracted from the invariant mass (m_{inv}) distributions of $K^+ + K^-$ candidates after subtraction of combinatorial background estimated using event mixing [8]. A momentum dependent residual background due to correlated pairs from the same event remains after the background subtraction. The kaons were identified through their dE/dx energy loss in the STAR TPC [23]. Accounting for the detector resolution, the values of the reconstructed ϕ mass and width are consistent with the PDG values [24]. The relative systematic uncertainty due to the dE/dx cut was estimated to be $\sim 8\%$ by using different cuts and comparing the yields after a particle identification efficiency correction. Uncertainty in the residual background shape of the m_{inv} distributions resulted in a contribution of about 4.5% to the errors on the final yields.

The ϕ -meson v_2 results were obtained using the v_2 vs m_{inv} method described in Ref. [25]. The method involves calculating the v_2 of the same-event distribution as a function of m_{inv} and then fitting the resulting $v_2(m_{inv})$ distribution using

$$v_2(m_{inv}) = v_{2S}\alpha(m_{inv}) + v_{2B}(m_{inv})[1 - \alpha(m_{inv})], \quad (1)$$

where $v_{2S} \equiv v_{2\phi}$ is the signal v_2 and v_{2B} is the background v_2 . $\alpha(m_{inv}) = S/(S + B)$ is the ratio of the signal over the sum of the signal plus background of the m_{inv} distributions. It was extracted from fits (Breit-Wigner plus a linear function) to the ϕ mass peak for each p_T bin. For each p_T bin, the $v_2(m_{inv})$ was fitted using Eq. (1) in order to extract the fitting parameter v_{2S} and v_{2B} was parameterized using a linear or quadratic function in m_{inv} . These results are consistent with results using an established method [26] where the ϕ -meson yield is studied as a function of the difference between its azimuthal angle and the estimated reaction plane angle, $(\phi - \Psi)$.

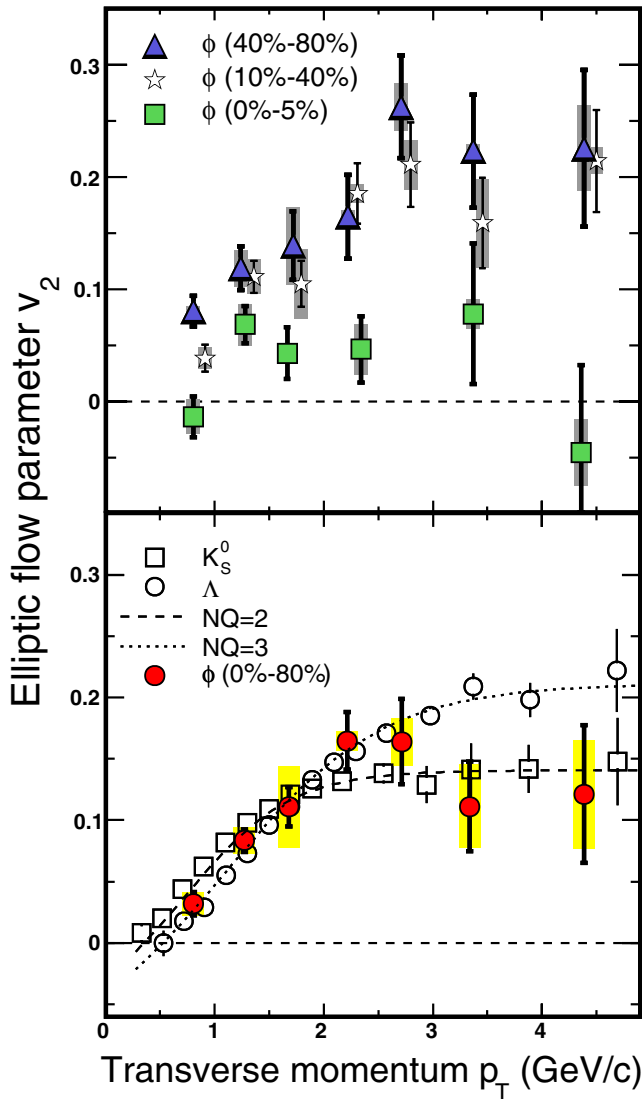


FIG. 1 (color online). Top panel: The elliptic flow, $v_2(p_T)$, for the ϕ -meson as a function of centrality. The vertical error bars represent the statistical errors while the shaded bands represent the systematic uncertainties. For clarity, data points are shifted slightly in p_T . Bottom panel: Minimum bias $v_2(p_T)$ for the ϕ -meson compared to results for Λ and K_S^0 [12]. The dashed and dotted lines represent parameterizations inspired by number-of-quark scaling ideas from Ref. [29] for $NQ = 2$ and $NQ = 3$, respectively.

In the top panel of Fig. 1 we present the first measurement of the differential elliptic flow, $v_2(p_T)$, of the ϕ meson from Au + Au collisions for three centrality bins. In this and the following figures, the vertical error bars on the ϕ data points indicate the statistical errors while the shaded bands indicate the extent of the systematic uncertainties. The systematic errors vary from point to point including uncertainties in extracting the signal for obtaining $\alpha(m_{\text{inv}})$ and differences in the reaction plane resolution determination. For minimum bias collisions, an additional contribution to account for the different methods of ex-

tracting the $v_2(p_T)$ values is also included in the systematic error. Nonflow effects [27,28] are not included in the systematic error. As expected, $v_2(p_T)$ increases with increasing eccentricity (decreasing centrality) of the initial overlap region. This trend is also illustrated in Table I which presents the p_T -integrated values of ϕ -meson elliptic flow, $\langle v_2 \rangle$, calculated by convoluting the $v_2(p_T)$ with the respective p_T spectrum for three centrality bins. It should be noted that the centrality dependence of the $\langle v_2 \rangle$ of ϕ -mesons is consistent with that of charged hadrons [28].

The lower panel of Fig. 1 shows the minimum bias (0%–80%) result compared to parameterizations for number-of-quark scaling for mesons ($NQ = 2$) and baryons ($NQ = 3$) whose free parameters have been fixed by fitting to the Λ and K_S^0 results simultaneously [29]. In this case, for $p_T < 2$ GeV/c, the ϕ v_2 follows a mass-ordered hierarchy where the values of v_2 , within errors, fall between those of the heavier Λ (open circles) and lighter K_S^0 (open squares). However, at intermediate p_T , between 2–5 GeV/c, the ϕ v_2 appears to follow the same trend as K_S^0 . When we fit the $v_2(p_T)$ of ϕ -mesons with the quark number scaling ansatz [29], the resulting fit parameter $NQ = 2.3 \pm 0.4$. The fact that the ϕ $v_2(p_T)$ is the same as that of other mesons indicates that the heavier s quarks flow as strongly as the lighter u and d quarks. As previously mentioned, ϕ -mesons are not formed through kaon coalescence [8] and do not participate strongly in hadronic interactions. Therefore the results provide evidence for partonic collectivity at RHIC.

Figure 2 shows the p_T distributions of ϕ -mesons for different centrality bins. The central-triggered dataset was used to obtain the most central spectrum while the other distributions were obtained using the minimum bias dataset. The error bars shown in Fig. 2 are statistical only. In the figure, the errors are smaller than the size of the data points.

Each p_T spectrum in Fig. 2 has been fitted using both an exponential function (dashed lines) in m_T and a Levy function [30] (dotted lines) which has an exponential-like shape at low p_T and is power-law-like at higher p_T . While the central data are fitted equally well by both functions the more peripheral spectra are better fitted by the Levy function indicating less thermal contributions in peripheral collisions.

In Fig. 3, the ratios of $N(\Omega)/N(\phi)$ vs p_T are presented for three centrality regions. The Ω data points are from Ref. [31] (for 0%–10%) and Ref. [32] for the other centralities. The errors of the ratios are dominated by the Ω data points. Also shown in the figure are recombination model expectations for central collisions [22] based on ϕ and Ω

TABLE I. Integrated elliptic flow, $\langle v_2 \rangle$, for the ϕ -meson for four centrality bins. The up- and low-error bars represent the statistical and systematic errors, respectively.

Centrality	40%–80%	10%–40%	0%–5%	0%–80%
$\langle v_2 \rangle$ (%)	$8.7^{+1.1}_{-0.02}$	$6.6^{+0.8}_{-0.2}$	$2.1^{+1.2}_{-0.5}$	$5.8^{+0.6}_{-0.2}$

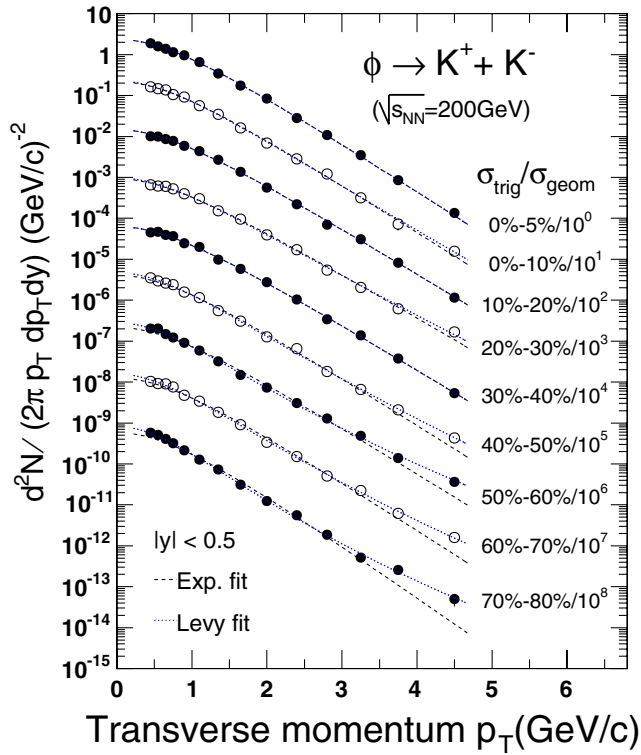


FIG. 2 (color online). Transverse momentum distributions of ϕ -mesons from Au + Au collisions at $\sqrt{s_{NN}} = 200$ GeV. For clarity, distributions for different centralities are scaled by factors of ten. Dashed lines represent the exponential fits to the distributions and the dotted lines are Levy function fits. Error bars represent statistical errors only.

production from coalescence of thermal s quarks in the medium. The model describes the trend of the data up to $p_T \sim 4$ GeV/c but fails at higher p_T . Other models based on dynamical recombination of quarks [20,33] were also compared to the data. However, Ref. [20] overpredicts the ratio while Ref. [33] gives the wrong shape. With decreasing centrality, the observed $N(\Omega)/N(\phi)$ ratios seem to turn over at successively lower values of p_T , indicating a smaller contribution from thermal quark coalescence in more peripheral collisions. This is also reflected in the smooth evolution of the spectra shapes from the thermal-like exponential to power-law shapes shown in Fig. 2.

The nuclear modification factor $R_{CP}(p_T)$ measures the change of p_T distributions from peripheral to central collisions and has been measured for most of the identified hadrons. It is the number of binary collision (N_{bin}) normalized ratio of the yields from central collisions over that from the peripheral collisions [12]. In Fig. 4, the high-statistics ϕ -meson R_{CP} (solid circles) is compared to K_S^0 (open triangles) and Λ (open squares) from Ref. [12] for two different centrality combinations (upper and lower panels). In both panels the binary-scaled yield of ϕ -mesons is suppressed (R_{CP} below unity) in central compared to peripheral collisions. It has been shown that u , d and s quarks are approaching equilibration at hadroniza-

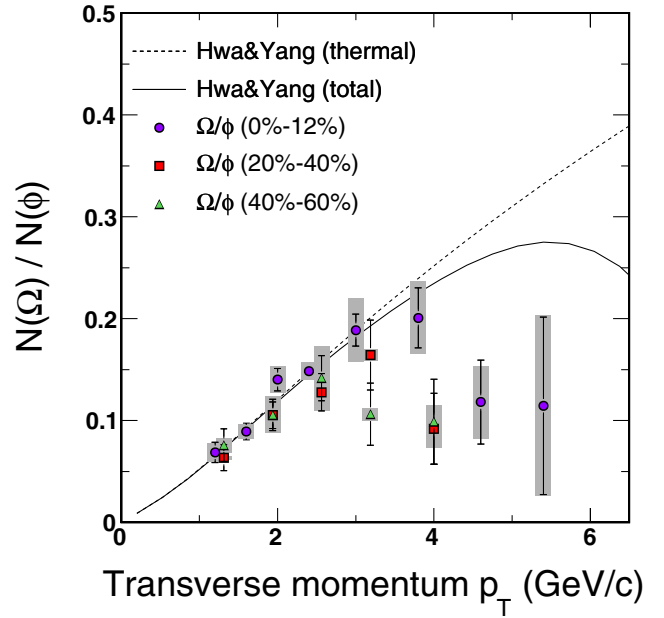


FIG. 3 (color online). The $N(\Omega)/N(\phi)$ ratio vs p_T for three centrality bins in $\sqrt{s_{NN}} = 200$ GeV Au + Au collisions. The solid and dashed lines represent recombination model predictions for central collisions [22] for total and thermal contributions, respectively. Note for the most central collision, the data of ϕ are Ω are from top 12% and 10%, respectively.

tion [31]. The ϕ -meson R_{CP} is more consistent with that of K_S^0 (meson) than of Λ (baryon) for the 0–5% vs 40–60% case (upper panel). This is as predicted by particle production models based on recombination of thermal quarks [20]. For the more peripheral bin (lower panel) the ϕ R_{CP} falls between that of the Λ and K_S^0 . In the 60–80% bin, the binary collision-scaled ϕ production is very similar to that in $p + p$ and $d + Au$ collisions where strangeness production is canonically suppressed [34]. Therefore a baryon-meson scaling behavior of R_{CP} is not expected in the lower panel of Fig. 4. In addition, for baryons and mesons, respectively, there seems to be an ordering in terms of strangeness content. This has also been observed in R_{AA} for strange particles [35].

In summary, we have presented first measurements of the elliptic flow of ϕ -mesons as a function of collision centrality in Au + Au collisions at $\sqrt{s_{NN}} = 200$ GeV. At low p_T (< 2 GeV/c), v_2 is consistent with hydrodynamical expectations. At intermediate p_T ($2 < p_T < 5$ GeV/c), v_2 of ϕ -mesons is consistent with number-of-quark scaling for mesons. These observations indicate the development of partonic collectivity in the medium. Measurements of the ϕ p_T spectra as a function of centrality show an evolution of the spectral shape from exponential to power-law-like with decreasing centrality, reflecting the increasing contributions from hard and possibly other non-equilibrium processes in more peripheral collisions. The result of a recombination model [22] is consistent with the trend of the central $N(\Omega)/N(\phi)$ ratio up to $p_T \sim 4$ GeV/c

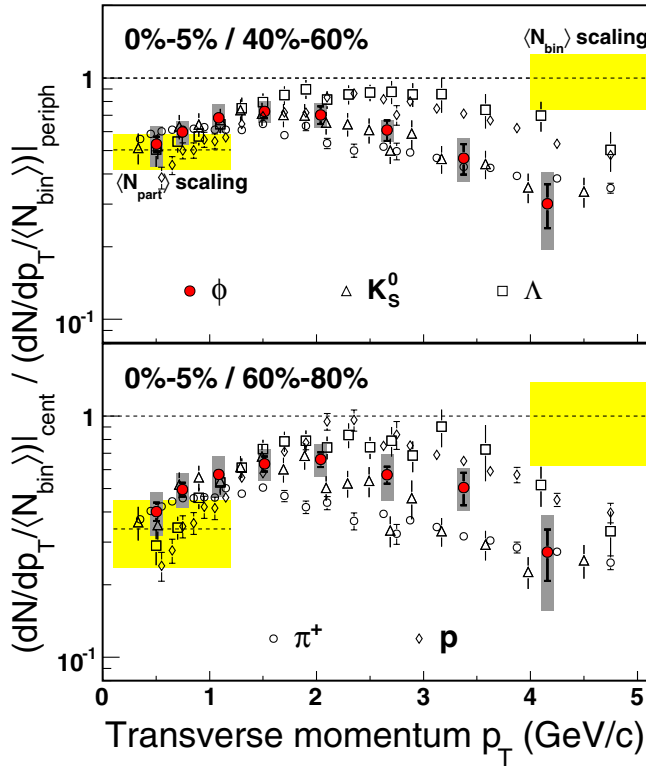


FIG. 4 (color online). The R_{CP} of midrapidity ϕ -mesons produced in $\sqrt{s_{NN}} = 200$ GeV Au + Au collisions: (top) 0%–5% vs 40%–60% and (bottom) 0%–5% vs 60%–80%. The shaded bands represent the uncertainties in the Glauber model calculations for $\langle N_{bin} \rangle$ and $\langle N_{part} \rangle$ [36]. Also shown are results for Λ and K_S^0 [12] and protons and π^+ [37].

which covers more than 95% of the hadron yields. At higher p_T , the model fails. The ϕ -meson R_{CP} resembles the K_S^0 for the 0%–5% vs 40%–60% case which is consistent with meson scaling. Since ϕ -mesons are made via coalescence of seemingly thermalized s quarks in central Au + Au collisions, the observations imply hot and dense matter with partonic collectivity has been formed at RHIC.

We thank the RHIC Operations Group and RCF at BNL, and the NERSC Center at LBNL for their support. This work was supported in part by the Offices of NP and HEP within the U. S. DOE Office of Science; the U. S. NSF; the BMBF of Germany; No. CNRS/IN2P3, RA, RPL, and EMN of France; EPSRC of the United Kingdom; FAPESP of Brazil; the Russian Ministry of Science and Technology; the Ministry of Education and the NNSFC of China; IRP and GA of the Czech Republic, FOM of the Netherlands, DAE, DST, and CSIR of the Government of India; Swiss NSF; the Polish State Committee for Scientific Research; SRDA of Slovakia, and the Korea

Sci. & Eng. Foundation. H.G.R. thanks the Alexander von Humboldt Foundation for generous support.

- [1] F. Karsch, Nucl. Phys. **A783**, 13 (2007).
- [2] Z. Fodor and S. D. Katz, Phys. Lett. B **534**, 87 (2002).
- [3] J. Phys. G **30**, S633 (2004); Nucl. Phys. **A774**, 1c (2006).
- [4] I. Arsene *et al.*, Nucl. Phys. **A757**, 1 (2005); B. B. Back *et al.*, Nucl. Phys. **A757**, 28 (2005); J. Adams *et al.*, Nucl. Phys. **A757**, 102 (2005); K. Adcox *et al.*, Nucl. Phys. **A757**, 184 (2005).
- [5] A. Shor, Phys. Rev. Lett. **54**, 1122 (1985).
- [6] T. Ishikawa *et al.*, Phys. Lett. B **608**, 215 (2005).
- [7] A. Sibirtsev, H.-W. Hammer, U.-G. Meissner, and A. W. Thomas, Eur. Phys. J. A **29**, 209 (2006).
- [8] J. Adams *et al.*, Phys. Lett. B **612**, 181 (2005); C. Adler *et al.*, Phys. Rev. C **65**, 041901(R) (2002).
- [9] J.-Y. Ollitrault, Phys. Rev. D **46**, 229 (1992).
- [10] H. Sorge, Phys. Rev. Lett. **82**, 2048 (1999).
- [11] J. Adams *et al.*, Phys. Rev. Lett. **95**, 122301 (2005) and references therein.
- [12] J. Adams *et al.*, Phys. Rev. Lett. **92**, 052302 (2004).
- [13] P. Huovinen, P. F. Kolb, U. Heinz, P. V. Ruuskanen, and S. A. Voloshin, Phys. Lett. B **503**, 58 (2001).
- [14] C. Nonaka *et al.*, Phys. Lett. B **583**, 73 (2004).
- [15] T. Hirano and Y. Nara, Phys. Rev. C **69**, 034908 (2004).
- [16] S. S. Adler *et al.*, Phys. Rev. Lett. **91**, 182301 (2003).
- [17] J. Adams *et al.*, Phys. Rev. C **71**, 064902 (2005).
- [18] S. A. Voloshin, Nucl. Phys. **A715**, 379c (2003).
- [19] D. Molnar and S. A. Voloshin, Phys. Rev. Lett. **91**, 092301 (2003).
- [20] R. J. Fries *et al.*, Phys. Rev. C **68**, 044902 (2003).
- [21] J. H. Chen *et al.*, Phys. Rev. C **74**, 064902 (2006).
- [22] R. Hwa and C.-B. Yang, arXiv:nucl-th/0602024v3.
- [23] K. H. Ackermann *et al.*, Nucl. Instrum. Methods Phys. Res., Sect. A **499**, 624 (2003).
- [24] Review of Particle Physics, J. Phys. G **33**, 1 (2006).
- [25] N. Borghini and J.-Y. Ollitrault, Phys. Rev. C **70**, 064905 (2004).
- [26] A. M. Poskanzer and S. A. Voloshin, Phys. Rev. C **58**, 1671 (1998).
- [27] C. Adler *et al.*, Phys. Rev. C **66**, 034904 (2002).
- [28] J. Adams *et al.*, Phys. Rev. C **72**, 014904 (2005).
- [29] X. Dong *et al.*, Phys. Lett. B **597**, 328 (2004).
- [30] J. Adams *et al.*, Phys. Lett. B **637**, 161 (2006).
- [31] J. Adams *et al.*, Nucl. Phys. **A757**, 102 (2005).
- [32] J. Adams *et al.*, Phys. Rev. Lett. **98**, 062301 (2007).
- [33] L.-W. Chen and C. M. Ko, Phys. Rev. C **73**, 044903 (2006).
- [34] A. Tounsi, A. Mischke, and K. Redlich, Nucl. Phys. **A715**, 565c (2003).
- [35] S. Salur (STAR Collaboration), Nucl. Phys. **A774**, 657c (2006).
- [36] J. Adams *et al.*, Phys. Rev. C **70**, 054907 (2004).
- [37] B. I. Abelev *et al.*, Phys. Rev. Lett. **97**, 152301 (2006).